The plasma crystal

M. H. Thoma,[a] M. Kretschmer, H. Rothermel, H. M. Thomas, and G. E. Morfill
Centre for Interdisciplinary Plasma Science, Max-Planck-Institut für Extraterrestrische Physik, P. O. Box 1312, 85741 Garching, Germany

(Received 29 June 2004; accepted 23 November 2004)

A complex plasma is a multi-component low-temperature plasma containing microparticles, for example, dust, in addition to ions, electrons, and neutral gas atoms. Under certain conditions these microparticles can form a regular structure, a plasma crystal. This new form of matter provides a unique possibility for studying phase transitions and dynamical aspects of many-body systems at the microscopic level. Complex plasmas play an important role in astrophysics as well as in technology. We describe an undergraduate experiment in which students can produce and investigate the plasma crystal and the transition to the liquid phase. © *2005 American Association of Physics Teachers.*
[DOI: 10.1119/1.1848515]

I. INTRODUCTION

The term ''plasma crystal'' might seem contradictory because plasmas are usually thought of as ionized gases. However, complicated structures can arise in a complex, multicomponent plasma containing microparticles such as dust, and for certain conditions the microparticles can arrange themselves in a lattice structure. A plasma crystal occurs because microparticles of the size of a few microns in a low temperature plasma collect up to 10^5 electron charges on their surface. Hence the microparticles interact strongly with each other by the Coulomb interaction. The formation of a plasma crystal occurs at a specific value of ratio Γ of the screened Coulomb energy to the thermal energy of the particles ($\simeq k_B T$):

$$\Gamma = \frac{Z^2 e^2 \exp(-a/\lambda_D)}{4\pi\epsilon_0 a k_B T}, \tag{1}$$

where Ze is the mean charge per particle, a the average distance between the particles, λ_D is the Debye screening length, and T is the temperature corresponding to the kinetic energy of the particles. Plasmas with $\Gamma > 1$ are called strongly coupled.[1,2] Crystallization takes place if the Coulomb coupling parameter Γ exceeds a certain value. For the one-component plasma with unscreened Coulomb interaction ($\lambda_D = \infty$) the critical value $\Gamma_c = 172$ was predicted by numerical simulations.[3]

In nature and in the laboratory strongly coupled plasmas are difficult to find because dense plasmas, corresponding to a small distance between the particles, and low temperatures are required to obtain a large value of Γ. However, under these conditions recombination sets in quickly and the plasma disappears. An alternative is multicomponent or complex plasmas, in which the microparticles, considered as a component of the plasma, receive a large charge Ze, which leads to a large value for Γ.

The plasma crystal was predicted as a new state in complex laboratory plasmas in 1986[4] and found experimentally at the Max Planck Institute for Extraterrestrial Physics in 1994.[5–7] The plasma crystal was immediately verified by other groups.[8–10] After the discovery of the plasma crystal, complex plasmas became a rapidly growing research field.[11] The interest in complex plasma physics is due not only to the discovery of the plasma crystal, but also due to its applications.[12] Complex plasmas are ideal model systems for studying phase transitions and dynamical aspects of many body systems at the microscopic level in real time.[13] Furthermore, there are several astrophysical situations, such as interstellar clouds, comets, planetary rings, and accretion disks, in which plasma-dust interactions play an important role. In semi-conductor technology where dust contamination is a serious problem, plasma etching is a standard method for producing microchips. Therefore, it is desirable to improve our understanding of dust-plasma interactions (for example, the origin and growth of dust particles and the forces on dust particles) as well as of the dust-dust interaction that can cause plasma crystal formation.

The plasma crystal table-top experiment can be easily used for educational purposes. In the following we will discuss the experimental set-up and implementation and the benefits of this experiment for teaching physics.

II. THE PLASMA CRYSTAL EXPERIMENT

A. Production of the complex plasma

The experimental set-up is shown in Fig. 1. The plasma is produced in a rf plasma chamber as sketched in Fig. 2. The plasma ignites in argon gas at room temperature and a pressure between 10 and 100 Pa by applying a rf power (13.56 MHz) of about 1.9 W to the circular electrodes at the bottom and the top of the plasma chamber. (The distance between the electrodes is 3 cm.) Before filling the chamber with gas, it should be evacuated by using a turbo molecular pump for several hours (base pressure $p \simeq 10^{-3}$ Pa) to guarantee perfect plasma conditions. (Oxygen contaminations can change the plasma conditions in a way that no crystal forms.) After the ignition of the plasma the rf power can be reduced to about 0.3 W to sustain the plasma. (The degree of ionization of this low temperature plasma is between 10^{-7} and 10^{-6}.) Finally, mono-disperse microparticles (melamine formaldehyde) with a diameter of 3.4 μm are injected into the plasma through the upper electrode via a particle dispenser. The pressure, rf voltage, and particle injection are controlled by dedicated software running on a personal computer.

B. Observation of the microparticles

The particles are observed by laser illumination through the glass windows of the plasma chamber, for which the pointlike laser source (diode laser, wavelength 686 nm, power 20 mW) is converted by a lens into a vertical sheet

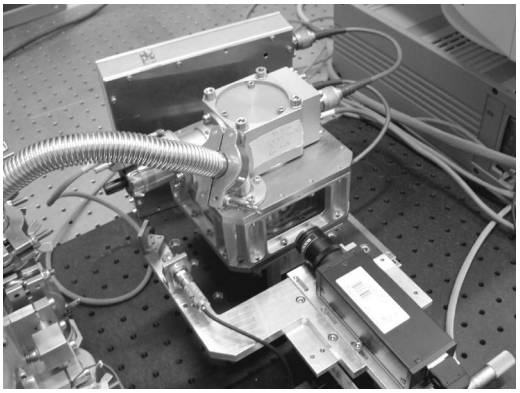

Fig. 1. Experiment setup: Plasma chamber with glass windows (center), particle dispenser (top), and camera and laser on translation stage (front).

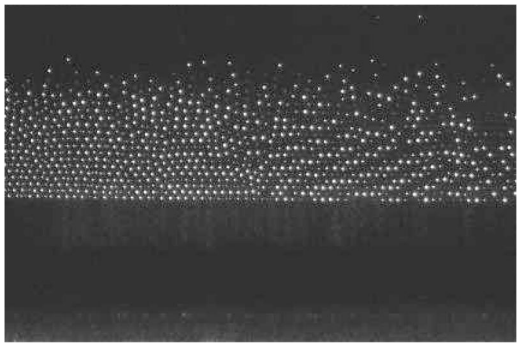

Fig. 3. Side view of the plasma crystal at 57 Pa recorded with a CCD camera. The hexagonal structures and lattice defects of the plasma crystal are shown. The laser width is thicker at the left side of the image, simulating a larger microparticle density there.

with a height of about 3 cm and a minimum thickness of about 100 μm. The laser light scattered from the microparticles (Mie scattering) is recorded in a second personal computer using a digital CCD camera. An interference filter (686 nm, 10 nm half width) is used in front of the camera lens to reject the plasma glow which accompanies the scattered light from the microparticles. The laser-camera system is mounted on a motor-driven translation stage which lets us perform scans. In this way the horizontal and three-dimensional structure of the plasma crystal can be determined.

C. Charging of the microparticles and formation of the plasma crystal

Immediately after the injection of the microparticles, they form a flat cloud a few millimeters above the lower electrode (see Fig. 3). As can be observed on the computer display, the microparticles start to form regular structures. The reason for this phenomenon is the following.

The temperature of the electron component is about 1–3 eV, whereas the ion temperature stays at the neutral gas temperature, that is, room temperature. Because of this effect and the small mass of the electrons, they exhibit a much higher mobility than the ions. Therefore the equilibrium charge on the microparticles, due to the balance of the electron and ion currents to the particle surface,[14] is typically of the order of 10^4 electron charges. In the plasma sheath extending a few millimeters above the lower electrode, there is a static electric field produced by space charges. Due to this field the charged microparticles are suspended against gravity in a narrow region above the lower electrode[15] as shown in Fig. 3. The entire plasma between the electrodes is surrounded by a static electric field, which confines the charged microparticles in the horizontal direction. This field makes possible the formation of the plasma crystal by the purely repulsive screened Coulomb force between the microparticles. The formation of the crystal at the initial pressure of 57 Pa takes only a few seconds, although the quality of the crystalline structure improves within a couple of minutes. The transition value for crystallization of a multi-component screened Coulomb system is the order of $\Gamma_c \simeq 1000$.[16]

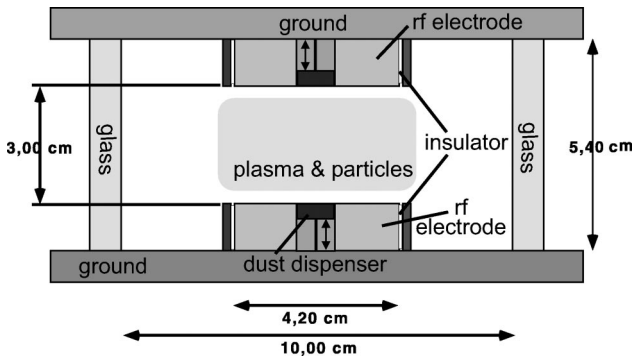

Fig. 2. Sketch of the plasma chamber, showing the dimensions and components of the rf plasma chamber used in the experiment.

D. Structures observed in the experiment

A visual inspection of the microparticles using the standard software available with the digital camera shows that there are about 20 horizontal layers. At the beginning the microparticles arrange in vertical chains. These strings arise from the interaction of charged grains with the positive ions streaming to the lower electrode in the electric field of the space charge. The ions are deflected by the microparticles, forming a positive charge cloud below them. This distortion of the Debye sphere around the microparticles leads to the observed stringlike configurations.[17] After a few minutes, during which the crystal stabilizes further, hexagonal structures also can be observed (see Fig. 3). At the edge of the electrodes vortices appear due to nonconservative forces, caused, for example, by microparticle charge variations in the presence of spatial variations of the electric field.[18]

The lattice distances and dimensions of the crystal can be extracted directly from the images on the computer display. The typical lattice distance is about 200 μm and the total number of microparticles typically used in the experiment is about 300 000. The distance increases with decreasing rf power because the ion density n_i decreases and therefore the Debye screening length $\lambda_D \sim n_i^{-1/2}$ increases, enhancing the repulsive force between the microparticles.

E. Determination of the lattice structure

From only the side view images, the crystal structure in the horizontal planes and the three-dimensional structure cannot be determined. Therefore a laser scan in the horizontal direction perpendicular to the field of view is performed. The camera and laser are mounted on a motor-driven translation stage that is controlled by a computer. We scanned through the crystal at a velocity of 0.3 mm/s, and recorded

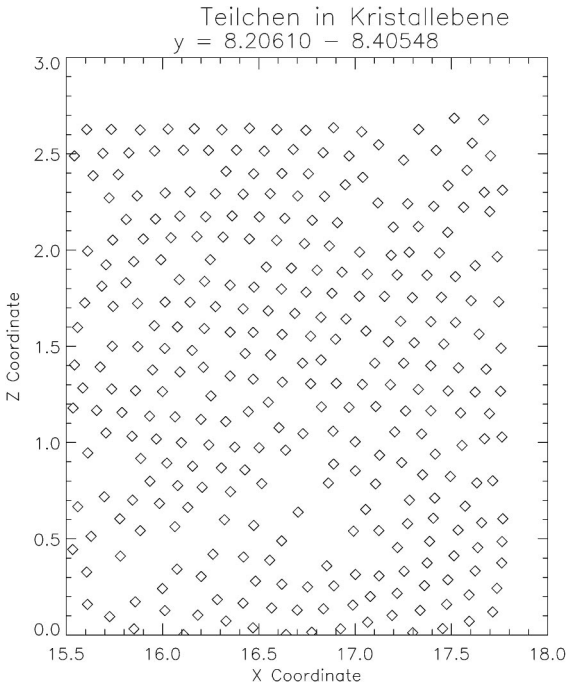

Fig. 4. Hexagonal lattice of the lowest horizontal plane obtained from a scan at 57 Pa. The voids are caused either by lattice defects or more likely by the selection criteria of the program.

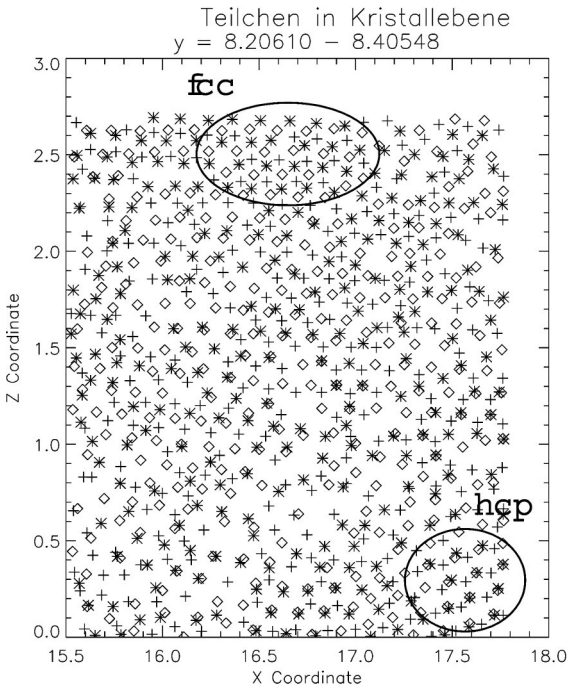

Fig. 5. Superposition of the three lowest planes at 57 Pa: lower plane (diamonds), middle plane (crosses), upper plane (stars). Domains in which the upper plane is on top of the lower correspond to a hcp lattice. Domains in which all three planes are in different places correspond to a fcc lattice.

100 vertical planes at a rate of 7.5 frames per second. These pictures are then analyzed by an IDL program[19] written for this purpose, and the microparticle positions are extracted in three dimensions. To investigate the three-dimensional structure, we restrict ourselves to a small volume containing only a few lattice layers with a horizontal extension of only about 20 lattice sites. Even with this restriction, the typical duration for computing the particle positions is 10–20 min. The particle positions are then displayed in each horizontal plane as shown in Fig. 4. Clearly a hexagonal structure can be observed. The voids are caused either by lattice defects or more likely by omitting particles due to the tracking criteria of the IDL program. (The program accepts particle positions only if the particle image exceeds a given brightness level and if a particle is found in at least three consecutive pictures.) The best crystal structure is found in the lowest plane, and the upper planes are more diffuse and have a less accurate crystal structure. The upper layers exert a pressure on the lower ones which improves the lattice structure.

Knowing the horizontal crystal structure does not uniquely determine the three-dimensional structure, because the hexagonal planar structure could belong either to a hcp or fcc lattice in three dimensions. The final structure can be decided by superimposing three consecutive layers. For a hcp configuration the third layer is on top of the first, corresponding to an ABABAB$\cdots$ordering. For fcc, where the horizontal planes are the (111)-planes, the ordering is ABCABC$\cdots$. As shown in Fig. 5, different domains containing hcp or fcc structures are found. This coexsistence of different crystal lattices indicates that both configurations have a similar free energy, and either structure is chosen randomly as soon as the crystal formation starts.[20]

F. Pair correlation function

The quality of the crystal can be investigated quantitatively by evaluating the pair correlation function.[6] The pair correlation function is defined as

$$g(r)=\left\langle \frac{1}{N}\sum_{i\neq j}^{N}\delta(\mathbf{r}-\mathbf{r_i}-\mathbf{r_j})\right\rangle, \tag{2}$$

where $\mathbf{r_i}$ and $\mathbf{r_j}$ are the position vectors of two particles and N is the total particle number. For a perfect crystal, the pair correlation function consists of sharp peaks corresponding to the distance to the nearest neighbors, to the next nearest neighbors, and so on. A typical result for the pair correlation function in the crystal phase is shown in Fig. 6. Several peaks can be clearly seen, indicating medium range order, that is, a crystal of rather high quality.

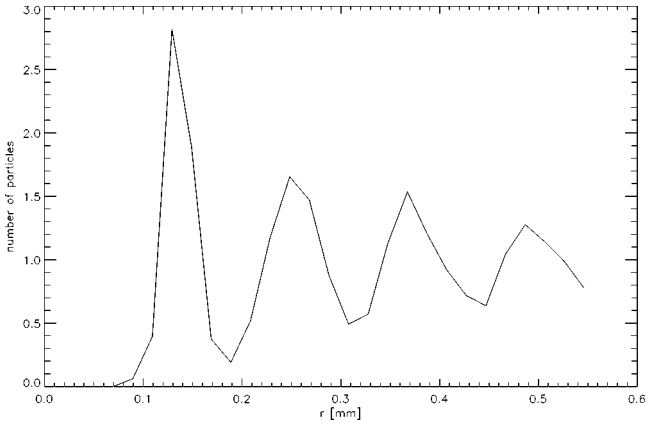

Fig. 6. Pair correlation function of the lowest plane at 57 Pa. The peaks correspond to the distance to the next neighbors, next nearest neighbors, etc. in the crystal. The peaks are broadened due to lattice defects and thermal fluctuations of the microparticles about their lattice sites.

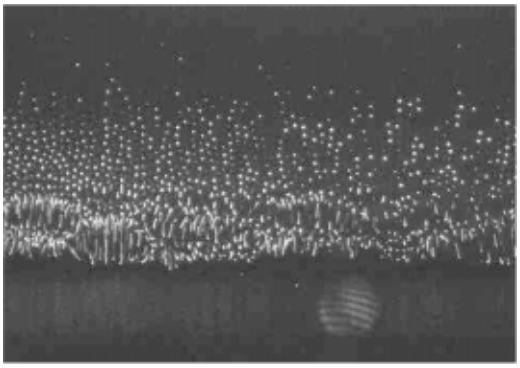

Fig. 7. Side view of the complex plasma at 23 Pa recorded with a CCD camera. In the lower part a dust-wave instability due to ion streaming is shown.

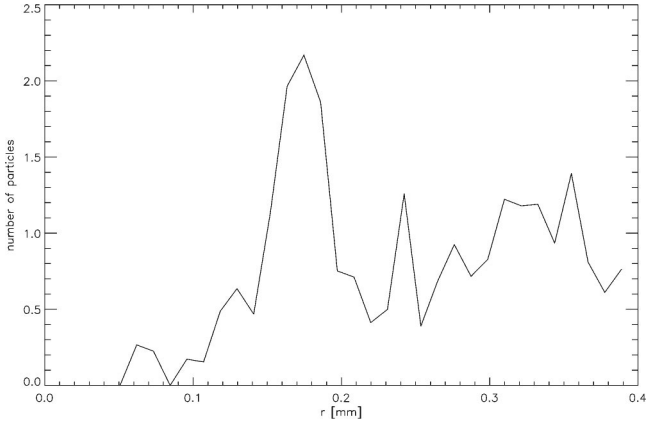

Fig. 8. Pair correlation function at 23 Pa. The large peak corresponds to the interparticle distance in the liquid phase of the complex plasma. The other peaks are caused by statistical fluctuations due to the limited number of microparticles.

G. Melting of the plasma crystal

In the next step of our experiment we reduce the pressure. In this way, both the electron temperature[21] and the friction of the microparticles in the neutral gas are reduced. Hence the charge on the particles is diminished and, at the same time, the kinetic temperature of the particles is increased. These effects lead to a reduction of the Coulomb coupling parameter and melting of the crystal if the critical value is reached.[6] Indeed, if the pressure is reduced, the crystal becomes more and more unstable. However, the ''melting'' of the crystal in our experiment occurs first due to another reason: if the pressure is lowered to about 30 Pa, a strong oscillation of the lower planes sets in (see Fig. 7). This turbulent particle motion is caused by a plasma instability. The origin of this instability can be traced back to the interaction of the microparticles with the ions streaming to the lower electrode. At lower pressure the ion mean free path, $\lambda_i \sim 1/p$, increases, and therefore also the ion velocity in the plasma sheath. If a critical value of the ion velocity is reached, a dust acoustic wave instability of the microparticle component sets in.[22] This instability shows up only in the lower planes, where the electric field of the plasma sheath is strong enough, and hence the ion velocity is sufficiently large. At pressures below 15 Pa, the entire particle system becomes unstable with large oscillation amplitudes.

As expected, a horizontal scan of the instability region does not show a regular structure. However, the pair correlation function still shows the first peak corresponding to the nearest neighbor distance (see Fig. 8). Such a correlation function describes an incompressible fluid, in which the distance to the nearest neighbor is constant (short range order); however, the distance to particles further away is random due to the streaming of the fluid.

III. CONCLUSIONS

Complex plasmas and the plasma crystal exhibit many interesting new phenomena and allow a large variety of interesting experiments. For example, we can investigate the phonon dispersion relations of the plasma crystal,[23] dust-plasma waves,[24] complex plasma boundaries and interfaces,[25] complex plasmas with different particle shapes, for example, rods,[26] shock waves[27] and Mach cones in complex plasmas,[28] small particle clusters,[29] plasma crystals in magnetic fields,[30] the thermophoretic suspension of microparticles,[31] particle growth[32] and coagulation,[33] complex plasmas in dc plasma chambers,[34] the forces acting on the particles,[35] and positively charged particles using UV light.[36] The particles can be observed directly by laser illumination and the dynamical behavior of the many-body system can be studied and analyzed in real-time. This property of complex plasmas offers the possibility of directly studying various aspects of plasma, solid-state, and fluid physics, for example, plasma waves and instabilities, crystallization, turbulent streaming, and also nonequilibrium properties of many-body systems such as self-organization. Therefore complex plasmas are an ideal subject for an undergraduate experimental physics course.

The experimental apparatus was first used for research purposes. The various components were built partly in our workshop, in particular the plasma chamber, the electronic control rack, the gas-vacuum system, and the translation stage for the camera-laser system. Other parts were purchased, such as the camera, the laser, the control and analysis computer, and the pumps. Readers interested in doing this experiment may contact the authors for further information. Detailed instructions for students at the Max-Planck-Institute can be found on the internet.[37]

Complex plasma experiments also have been performed under microgravity conditions on the International Space Station, where the disturbing influence of gravity on the microparticles is avoided.[38] New complementary experiments are planned and will be performed in laboratories on earth as well as the Space Station.

ACKNOWLEDGMENTS

We would like to thank M. Schwabe and M. Zuzic for writing and providing the IDL program used in this experiment and K. Tarantik for helping us with assembling the experimental apparatus. M.H.T. was supported by DLR (BMBF) under Grant No. 50WM0038 and M. K. under Grant No. 50WP0204.

[a)]Electronic mail: thoma@mpe.mpg.de

[1]S. Ichimaru, ''Strongly coupled plasmas: High-density classical plasmas and degenerate electron fluids,'' Rev. Mod. Phys. **54**, 1017–1059 (1982).
[2]W. Kraeft and M. Schlanges (ed.), *Physics of Strongly Coupled Plasmas* (World Scientific, Singapore, 1996).
[3]W. L. Slattery, G. D. Doolen, and H. E. Witt, ''Improved equation of state for the classical one-component plasma,'' Phys. Rev. A **21**, 2087–2095 (1980).

[4]H. Ikezi, ''Coulomb solid of small particles in plasmas,'' Phys. Fluids **29**, 1764–1766 (1986).
[5]H. Thomas, G. E. Morfill, V. Demmel, J. Goree, B. Feuerbacher, and D. Möhlmann, ''Plasma crystal: Coulomb crystallization in a dusty plasma,'' Phys. Rev. Lett. **73**, 652–655 (1994).
[6]H. Thomas and G. E. Morfill, ''Melting dynamics of a plasma crystal,'' Nature (London) **379**, 806–809 (1996).
[7]G. E. Morfill, H. M. Thomas, U. Konopka, and M. Zuzic, ''The plasma condensation: Liquid and crystalline plasmas,'' Phys. Plasmas **6**, 1769–1780 (1999).
[8]J. H. Chu and I. Lin, ''Direct observation of Coulomb crystals and liquids in strongly coupled rf dusty plasmas,'' Phys. Rev. Lett. **72**, 4009–4012 (1994).
[9]Y. Hayashi and K. Tachibana, ''Observation of Coulomb-crystal formation from carbon particles grown in a methane plasma,'' Jpn. J. Appl. Phys. **33**, L804–L806 (1994).
[10]A. Melzer, T. Trottenberg, and A. Piel, ''Experimental determination of the charge on dust particles forming Coulomb lattices,'' Phys. Lett. A **191**, 301–308 (1994).
[11]For reviews on complex plasmas see P. K. Shukla, D. A. Mendis, and V. W. Chow, *The Physics of Dusty Plasmas* (World Scientific, Singapore, 1996); V. N. Tsytovich, ''Dust plasma crystals, drops, and clouds,'' Phys. Usp. **40**, 53–94 (1997); A. Melzer, *Der Plasmakristall: Phasenübergang und Stabilität* (Harri Deutsch, THUN, 1997); A. Bouchoule, editor, *Dusty Plasmas* (Wiley, Chichester, 1999); P. Shukla, ''A survey of dusty plasma physics,'' Phys. Plasmas **8**, 1791–1803 (2001); V. N. Tsytovich, G. E. Morfill, and H. Thomas, ''Complex plasmas: I. Complex plasmas as unusual state of matter,'' Plasma Phys. Rep. **28**, 675–707 (2002); ''Complex plasmas: II. Elementary processes in complex plasmas,'' *ibid.* **29**, 3–36 (2003).
[12]R. L. Merlino and J. A. Goree, ''Dusty plasmas in the laboratory, industry, and space,'' Phys. Today **57**(7), 32–38 (2004).
[13]Colloids are also used for investigating crystallization and other dynamical processes. See, for example, C. A. Murray and D. G. Grier, ''Colloidal crystals,'' Am. Sci. **83**, 238–245 (1995). However, due to the large damping in those systems, the processes are much slower, often taking months to complete.
[14]T. Matsoukas and M. Russell, ''Particle charging in low-pressure plasmas,'' J. Appl. Phys. **77**, 4285–4292 (1995).
[15]Only under microgravity are microparticles present in the bulk plasma. Under gravity the microparticles are restricted to the plasma sheath. See G. E. Morfill, H. M. Thomas, U. Konopka, H. Rothermel, M. Zuzic, A. Ivlev, and J. Goree, ''Condensed plasmas under microgravity,'' Phys. Rev. Lett. **83**, 1598–1601 (1999).
[16]S. Hamaguchi, R. T. Farouki, and D. H. E. Dubin, ''Triple point of Yukawa systems,'' Phys. Rev. E **56**, 4671–4682 (1997).
[17]P. K. Shukla and N. N. Rao, ''Coulomb crystallization with streaming ions and dust grains,'' Phys. Plasmas **3**, 1770–1772 (1996).
[18]G. E. Morfill, H. M. Thomas, U. Konopka, H. Rothermel, M. Zuzic, A. Ivlev, and J. Goree, ''Condensed plasmas under microgravity,'' Phys. Rev. Lett. **83**, 1598–1601 (1999).
[19]⟨http://www.rsinc.com/idl⟩. The IDL code used in the experiment is available on request.
[20]M. Zuzic, A. V. Ivlev, J. Goree, G. E. Morfill, H. Rothermel, U. Konopka, R. Sütterlin, and D. D. Goldbeck, ''Three-dimensional strongly coupled plasma crystal under gravity conditions,'' Phys. Rev. Lett. **85**, 4064–4067 (2000).
[21]Decreasing the pressure in an Argon rf discharge, an abrupt reduction of the electron temperature from about 4 to 1 eV at about 40 Pa was reported and attributed to a change from stochastic to collisional electron heating. See V. A. Godyak and R. B. Piejak, ''Abnormally low electron energy and heating-mode transition in a low-pressure Argon rf discharge at 13.56 MHz,'' Phys. Rev. Lett. **65**, 996–999 (1990).
[22]M. Rosenberg, ''Ion- and dust-acoustic instabilities in dusty plasmas,'' Planet. Space Sci. **41**, 229–233 (1993).
[23]S. Nunomura, J. Goree, S. Hu, X. Wang, and A. Bhattarcharjee, ''Dispersion relations of longitudinal and transverse waves in two-dimensional screened Coulomb crystals,'' Phys. Rev. E **65**, 066402-1–11 (2002).
[24]A. Barkan, R. L. Merlino, and N. D'Angelo, ''Laboratory observation of the dust-acoustic wave mode,'' Phys. Plasmas **2**, 3563–3565 (1995).
[25]B. M. Annaratone, S. A. Khrapak, P. Bryant, G. E. Morfill, H. Rothermel, H. M. Thomas, M. Zuzic, V. E. Fortov, V. I. Molotkov, A. P. Nefedov, S. Krikalev, and Y. P. Semenov, ''Complex-plasma boundaries,'' Phys. Rev. E **66**, 056411-1–4 (2002).
[26]V. I. Moltkov, A. P. Nefedov, M. Y. Pustyl'nik, V. M. Torchinsky, V. E. Fortov, A. G. Khrapak, and K. Yoshino, ''Liquid plasma crystal: Coulomb crystallization of cylindrical macroscopic grains in a gas-discharge plasma,'' JETP Lett. **71**, 102–105 (2000).
[27]Y. Nakamura, H. Bailung, and P. K. Shukla, ''Observation of ion-acoustic shocks in a dusty plasma,'' Phys. Rev. Lett. **83**, 1602–1605 (1999).
[28]D. Samsonov, J. Goree, Z. W. Ma, A. Bhattacharjee, H. M. Thomas, and G. E. Morfill, ''Mach cones in a Coulomb lattice and a dusty plasma,'' Phys. Rev. Lett. **83**, 3649–3652 (1999).
[29]W.-T. Juan, Z.-H. Huang, J.-W. Hsu, Y.-J. Lai, and I. Lin, ''Observation of dust Coulomb clusters in a plasma trap,'' Phys. Rev. E **58**, R6947–R6950 (1998).
[30]D. Samsonov, S. Zhdanov, G. Morfill, and V. Steinberg, ''Levitation and agglomeration of magnetic grains in a complex (dusty) plasma with magnetic field,'' New J. Phys. **5**, 24(1–10) (2003).
[31]H. Rothermel, T. Hagl, G. E. Morfill, M. H. Thoma, and H. M. Thomas, ''Gravity compensation in complex plasmas by application of a temperature gradient,'' Phys. Rev. Lett. **89**, 175001-1–4 (2002).
[32]A. Bouchoule and L. Boufendi, ''Particulate formation and dusty plasma behaviour in argon-silane RF discharge,'' Plasma Sources Sci. Technol. **2**, 204–213 (1993).
[33]A. V. Ivlev, G. E. Morfill, and U. Konopka, ''Coagulation of charged microparticles in neutral gas and charge-induced gel transition,'' Phys. Rev. Lett. **89**, 195502-1–4 (2002).
[34]V. E. Fortov, A. P. Nefedov, V. M. Torchinskii, V. I. Molotkov, A. G. Khrapak, O. F. Petrov, and K. F. Volykhin, ''Crystallization of a dusty plasma in the positive column of a glow discharge,'' JETP Lett. **64**, 92–98 (1996).
[35]C. Zafiu, A. Melzer, and A. Piel, ''Ion drag and thermophoretic forces acting on free falling charged particles in an rf-driven complex plasma,'' Phys. Plasmas **9**, 4794–4803 (2002).
[36]V. N. Tsytovich, A. P. Nefedov, V. E. Fortov, O. F. Petrov, and G. E. Morfill, ''Effects of ultraviolet radiation on dusty plasma structures at microgravity,'' Phys. Plasmas **10**, 2633–2642 (2003).
[37]⟨http://cern.ch/thoma⟩ or ⟨http://www.physik.tu-muenchen.de/studium/betrieb/praktika/fopra⟩.
[38]A. P. Nefedov, Gregor E. Morfill, Vladimir E. Fortov, Hubertus M. Thomas, Hermann Rothermel, Tanja Hagl, Alexei V. Ivlev, Milenko Zuzic, Boris A. Klumov, Andrey M. Lipaev, Vladimir I. Molotkov, Oleg F. Petrov, Yuri P. Gidzenko, Sergey K. Krikalev, William Shepherd, Alexandr I. Ivanov, Maria Roth, Horst Binnenbruck, John A. Goree, and Yuri P. Semenov, ''PKE-Nefedov: plasma crystal experiments on the International Space Station,'' New. J. Phys. **5**, 33(1–10) (2003).